Profiling of micrometer-sized laser beams in restricted volumes

Yevhen Miroshnychenko, Otto Nielsen, Aske Thorsen, and Michael Drewsen*

QUANTOP, Danish National Research Foundation Center for Quantum Optics, Department of Physics and Astronomy, University of Aarhus, DK-8000 Aarhus C, Denmark

*Corresponding author: drewsen@phys.au.dk

Received 1 November 2011; revised 19 February 2012; accepted 24 February 2012; posted 24 February 2012 (Doc. ID 157467); published 25 April 2012

We present a method for determining the three-dimensional intensity distribution of directed laser radiation with micrometer resolution in restricted volumes. Our method is based on the incoupling and guiding properties of optical fibers, with the current version requiring only a few hundred micrometers across the measuring volume. We characterize the performance of the method and experimentally demonstrate profiling of micrometer-sized laser beams. We discuss the limiting factors and routes toward a further increase of the resolution and beam profiling in even more restricted volumes. Finally, as an application example, we present profiling of laser beams inside a micro ion trap with integrated optical fibers. © 2012 Optical Society of America

OCIS codes: 120.3940, 140.3295, 060.2370, 060.4005, 130.0130, 020.0020.

1. Introduction

A method for measuring the three-dimensional (3D) intensity distribution of directed laser radiation in a volume-restricted environment may be of importance in many different laser-light-based fields of industry and science. For example, it would allow for diagnostics of optical communication devices (e.g., fiber multiplexers [1]), including fast diagnostics during the research and development phase, manufacturing, final quality control, and service of such devices. Microbeam profiling may as well be an important tool in connection with optical data storage, e.g., [2], where extremely focused and high quality laser beams are needed and quick high quality beam diagnostics in restricted volumes is essential. Another example is multiphoton Raman spectroscopy [3], where several focused laser beams with required sizes should be carefully overlapped in space. Furthermore, in the fast growing field of experimental quantum optics, miniaturization of atomic particle traps with integrated optical elements, e.g., micro-optical resonators and optical waveguides, plays one of the key roles [4,5]. In such experimental configurations, it is desirable to know to a high degree the characteristics of the beams emerging after the integrated optics. Although there are many commercially available solutions for beam profiling, none of them so far has allowed performing the beam characterization *in situ* in restricted environments to check the quality of the assembly and characterize the optical part of the integrated system.

Existing directed laser radiation profiling techniques can be divided into three classes. The first class is based on direct projection of the whole laser beam onto a two-dimensional array of photosensitive pixels, such as photodiodes or a CCD chip for the following profile analysis [6]. The second class is based on a controlled shading of the laser radiation and recording the corresponding intensity reduction of the uncut beam. The shading can be done using a knife edge [7], a translating slit [8], a pinhole [9,10], a rotating mirror [11], or a wire [12]. The third class is based on spectroscopic [13,14] or thermographic [15,16] methods. The first two classes in the present form require bulky detectors in the vicinity of the measuring point both in the radial and axial extensions. The latter

1559-128X/12/132341-05$15.00/0

class, additionally, is based on properties of a medium around the measured laser beam and, therefore, is applicable only for special types of lasers.

Here we present a beam profiling method allowing micrometer resolution and requiring available "working volumes" of at most only several hundred micrometers across around the measuring position, which is enough to introduce our detector head based on the optical fiber. Additionally, the same method can be used to find the intersection point of several directed laser radiation sources even in volumes with restricted access to the laser beams. Finally, the micrometer resolution enables us to use the device for pointing stability measurements of directed laser radiation.

2. Principle of Operation

The scanning part of our probe is a slanted tip of an optical fiber; see Fig. 1. Directed laser radiation enters the fiber from the side. The operation of our beam probe is based on the interplay of three physical effects. First, the polished side of the optical fiber acts as a mirror to guide the light into the mode of the optical fiber; see the inset of Fig. 1. Second, at the fiber tip interface, laser radiation from only a micrometer-sized area is coupled into the guiding mode of the fiber. Finally, the coupled light is guided to a remote photodetector. This results in an electrical signal proportional to the laser radiation intensity at the position of the fiber tip. By scanning the position of the probe tip, one can reconstruct the 3D profile of the laser radiation pattern.

The efficient side incoupling into the fiber probe can be done either by using reflection coating of the polished surface or relying on total internal reflection (TIR) on the glass–air (vacuum) interface. The last method does not require extra coating, but only polishing at the proper angle θ. If the beam incoupling angle α (see the inset of Fig. 1) is larger than the critical angle for TIR, then just polishing of the fiber is enough to ensure reflection and does not require expensive reflection coating. Ideally, the reflecting side should be at exactly $\theta = 45°$, but the TIR condition is not satisfied at this angle for all silica optical fibers in air at typical wavelengths. Additionally, since at the border of the TIR condition the reflection is polarization sensitive, it is desirable to work in a deep TIR regime to avoid sensitivity to slight misalignments.

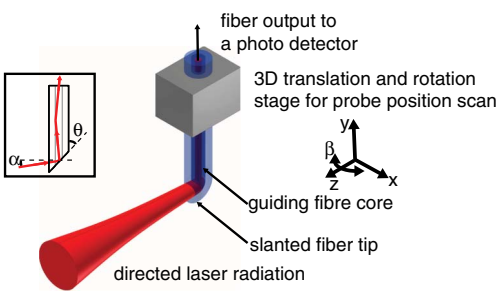

Fig. 1. (Color online) Principle of operation of the laser beam probe.

The area above the red (middle solid) line in Fig. 2(a) shows the calculated TIR region for a multimode fiber GIF62.5 at 866 nm. The reflected light should, at the same time, be within the numerical aperture of the optical fiber in order to be coupled into the fiber guiding mode; see the area between the blue (the upper and lower solid) lines in Fig. 2(a). The nonzero overlap between the two areas allows us to satisfy these light-incoupling conditions simultaneously; see the gray area in Fig. 2(a). In particular, we use the region around $\alpha = 0°$ during the operation of our probe. Therefore, as far as we reach the TIR regime, the spatial selectivity of our probe is polarization insensitive and is mainly defined by the incoupling efficiency into an optical fiber.

Generally, profiles recorded with this technique are convolutions of a beam shape with a transmission function (TF) of the scanning probe. In the simplest case of coupling light from a free propagating Gaussian beam into a normal cut single-mode fiber, the TF of the probe is well approximated by a Gaussian [17]. Assuming that the slanted end of the fiber works just as a mirror (neglecting the lensing effect of the curved entrance surface [18]), the corresponding transmission of the fiber probe as the function of the displacement d in the x–y plane at the beam waist is an overlap between the incoming beam and the fiber guiding mode:

$$T(d) = \frac{4w_b^2 w_f^2}{(w_b^2 + w_f^2)^2} \exp\left(-\frac{2d^2}{w_b^2 + w_f^2}\right),$$

where w_f is the effective width of the fiber probe TF, and w_b is the beam size along this scan direction (all beam sizes are given as a $1/e^2$ radius). The resulting profile has a Gaussian shape with the effective width $w_p = (w_b^2 + w_f^2)^{1/2}$. Consequently, the smaller is w_f, relative to the beam size, the tinier is the contribution from the convolution.

At the same time, the amount of transmitted light drops with the reduction of w_f. Much higher coupling efficiency can be reached with a multimode fiber. In this case the efficiency is given by an overlap between the incoming beam and all guiding modes of the fiber. Generally, it is quite difficult to analytically

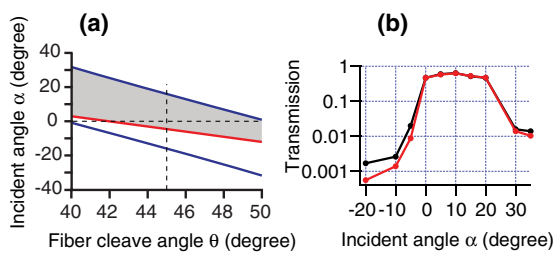

Fig. 2. (Color online) Light coupling into a fiber probe through a slanted tip. (a) Calculated high coupling region (gray) as the function of the fiber polishing angle θ and the incident angle α. (b) Measured transmission of a 22 μm waist beam at $\lambda = 866$ nm through a fiber probe with $\theta = 45°$ for the vertical (red lower curve) and the horizontal light polarizations (black upper curve).

account for all the guiding modes of a multimode fiber. Therefore, it is more practical to directly calibrate the width measured with such a fiber probe using some independent method, for example, a knife edge; see Fig. 4. This method is based on controlled shading of the beam with recording of the unshaded pattern and comparison to a beam model. Although this method requires an assumption about the beam shape and does not allow measurements in restricted volumes, it can be used for one time calibration of our probe using free propagating Gaussian beams. Such calibration once performed, can be used in all further measurements with this probe.

3. Characterization of the Probe

The central point of our fiber-based profiler is a slanted tip of an optical fiber, which is made by grinding the fiber tip at the desired angle. In order to have high control over the polishing angle, the fiber was mounted onto a special support tool; see Fig. 3. The main part of the tool is a precisely machined three-angular corner piece from aluminum. Thin glass plates are flat fixed to the slanted edge and to the bottom of the corner. The first plate provides a rigid support for the fiber, which is fixed on the glass plate using adhesive Crystal-bond (SPI Supplies). The second plate allows us to place the support tool directly onto the grinding ring (Struers). The grinding is performed in several steps with subsequent reduction of the grain size of the grinder ring. After the final step, the fiber can be safely removed from the support tool by chemically dissolving the Crystal-bond and subsequently clamped onto a translation stage holder.

In our tests we have used a high speed photodetector with a fiber connector DET63A from Thorlabs for light detection. Generally, any photodetector that matches the sensitivity in the spectral region of interest and the speed of the probe tip scan can be used. The 3D scan was performed using a translation stage with computerized motion in the x and y directions using 9065-XY from New Focus and manual in the z direction using PT1/M from Thorlabs, allowing a scan range of more than 15 mm in each direction. The x–y-translation stages were driven by Picomotors from New Focus with a step size of ~30 nm at the maximum speed of 2000 steps per second. In order to precisely track the motion of the fiber probe, we used miniature Michelson interferometers integrated on each translation stage. This allowed us to track the translation stages positions in the x and y directions with the precision of about 0.5 μm in each direction. Generally, one needs the position tracking precision to be at least 1 order of magnitude smaller than the size of the beam being characterized in order to have enough points for data processing. Note that closed-loop translation stages can be used to increase the precision, although at the expense of the scan speed.

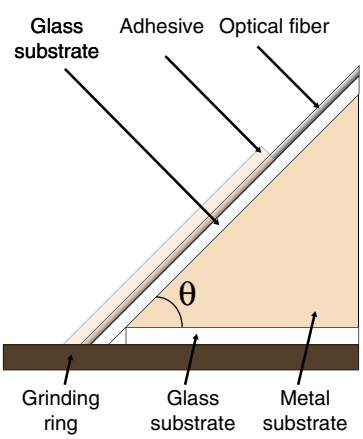

Fig. 3. (Color online) The tip of an optical fiber is ground at a desired angle θ using a special support tool.

Depending on the laser beam sizes, fiber beam profilers can be based on fibers with different core sizes. For beam sizes larger than ~20 μm one can choose multimode fibers with core diameters of several tens of micrometers, whereas for smaller beam sizes one can choose single-mode fibers. We have manufactured and characterized several of such fiber probes.

We first characterized the properties of a fiber beam profiler based on a multimode fiber GIF62.5 with $\theta = 45°$, which corresponds to the vertical dashed line in Fig. 2(a). Figure 2(b) shows a measured transmission as the function of the incoupling angle α for two light polarizations. We clearly observe strong polarization dependence for $\alpha < -5°$ as we approach the TIR edge and polarization independence for higher angles.

Second, we manufactured a probe based on the same fiber but with $\theta = 46°$, allowing us to reliably profile beams at an angle $\alpha = 0°$. We used this probe to measure radial profiles of three beams with different waists. These beams were independently characterized using the knife edge method to perform the calibration of the probe. In order to extract each waist in each direction, we performed 3D profiling of every beam. A series of x and y scans were carried out for different z positions. Each individual scan was repeated on average six times to estimate statistical deviations. The waists of the corresponding beams measured with the two techniques presented in Fig. 4. Since the measured beam size is a convolution of the original beam shape with the TF, for beam sizes comparable with the fiber core radius of 31.25 μm we observe deviation from the curve with

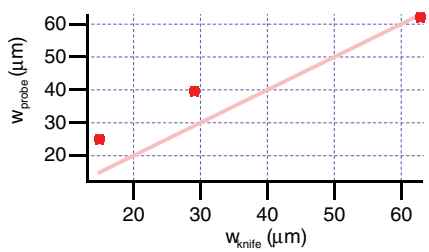

Fig. 4. (Color online) Beam waists of three beams measured with the multimode fiber probe along the x axis, compared to the knife edge method. The error bars are comparable to the size of the dots. The solid line with the slope 1 corresponds to a probe with infinitely small fiber core size.

the slope 1, corresponding to a probe with infinitely narrow TF. At the same time, for larger beam sizes this deviation is negligible.

Third, to demonstrate the operation of a beam profiler based on a single-mode fiber, we manufactured a probe with $\theta = 46°$ based on a fiber SM800-5.6-125 with the effective core radius $w_f = 2.9$ μm at 866 nm. For this small w_f the contribution from the convolution is below 10%, even for beams as small as $w_b = 6.5$ μm. Figure 5 shows the beam waists measured with this probe, compared to the knife edge method. Indeed, now we do not see in the measured range any significant deviations from the line with the slope 1, corresponding to infinitely small core radius. Figure 6(a) shows beam sizes along the y direction as the function of the axial z position along the beam. Figures 6(b)–6(d) give an example of the data from individual scans. After each scan the corresponding curve is fitted with a Gaussian to extract the beam size. Each point in Fig. 6(a) corresponds to an average of about six beam size measurements. The measured shape in Fig. 6(a) is in perfect agreement with the reference measurement using the knife edge method. For this beam we measure with the fiber probe waists $w_p^x = 15.0(4)$ μm and $w_p^y = 15.5(4)$ μm for the scans along the x and y directions. These waists agree quite well with corresponding knife edge measurements $w_b^x = 15.7(4)$ μm and $w_b^y = 15.7(4)$ μm, respectively. This demonstrates the feasibility of 3D profiling of micrometer-sized beams with single-mode fiber probes. Although we have only demonstrated profiling of Gaussian beams, our method allows us to characterize other beam shapes, for we do not need any *a priori* assumptions about the beam shape to reconstruct it from the measured data. If the beam size is much larger than the fiber core, no extra deconvolution is necessary, as we demonstrated in the last example. Otherwise the knowledge of the probe TF, e.g., Figs. 4 and Fig. 5, is enough to perform a deconvolution of an arbitrary beam shape. This demonstration is beyond the scope of this experimental work.

Finally, we experimentally verified the possibility to couple light into the probe not only directly at $\beta = 0°$ (see Fig. 1) but at different angles. The maximum

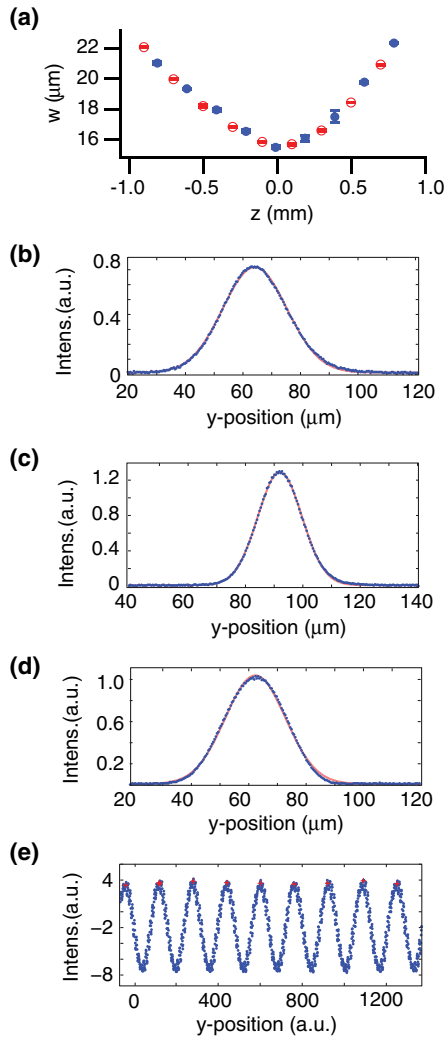

Fig. 6. (Color online) y-direction scans of the beam with a waist $w_b = 15.7$ μm. (a) Beam sizes measured along the y direction at different z positions using the knife edge method (red circles) and the fiber probe (blue dots). Note that the centers of the curves were superimposed, since the z references of the two methods are different. (b) Signal of the fiber probe during the vertical scan (blue points) and the corresponding Gaussian fit to the data (red curve) at $z = 0.79$ mm, (c) at $z = -0.01$ mm, and (d) at $z = -0.81$ mm. Each point in these graphs is taken when the fringe from the corresponding Michelson interferometer reaches its maximum during the scan. (e) Example of the interferometer signal.

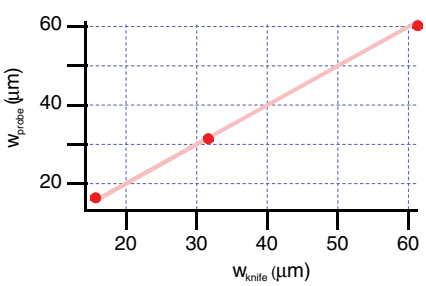

Fig. 5. (Color online) Beam waists of three beams measured with the single-mode fiber probe along the y direction, compared to the knife edge method. The error bars are comparable to the size of the dots. The solid line with the slope 1 corresponds to a probe with infinitely small fiber core size.

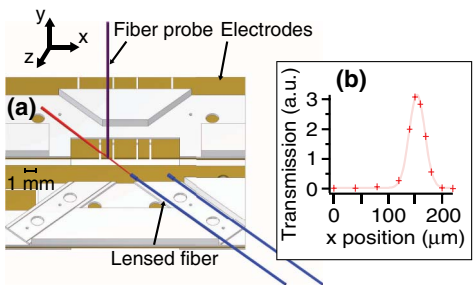

Fig. 7. (Color online) Probing beams from optical fibers integrated into a micro ion trap. (a) Schematic of a partly assembled Paul trap. The fibers are integrated between the layers of electrodes. The upper electrodes are not shown. (b) Example of a beam profile measured *in situ* inside the ion trap.

measured transmission through the multimode fiber probe is still 20% at $\beta = \pm 45°$, relative to the direct coupling. This result opens the possibility to use such a probe for free space beam overlap.

We have used our fiber probe based on the multimode fiber GIF62.5 for *in situ* characterization of beams from four single-mode lensed fibers inside a micro ion trap; see Fig. 7(a). Using this method, we aligned the fibers so that both beams are crossing at the center of the ion trapping region and characterized the beams afterward. Figure 7(b) shows an example of a one-dimensional scan through one of the beams at $\lambda = 397$ nm.

4. Conclusion and Outlook

We have presented and successfully experimentally tested a beam profiling method with micrometer resolution capable of working in spatially restricted environments. We tested the method for free propagating beams, where an independent knife edge technique is applicable, and found the results in good agreement using the independent methods. Our technique requires available "working volumes" of at most only several hundred micrometers across in the vicinity of the measuring position, which is enough to introduce our detector head. A further reduction of the working volume and increase of the resolution can be achieved by radial etching, tapering of the fiber, or structural coating of the incoupling tip.

The authors thank P. Balling for the discussions on the early stage of the project. We acknowledge financial support from the Danish National Research Foundation's Center for Quantum Optics (QUANTOP) (JNR. 02-512-44), the European Union (EU) Consortium Project MICROTRAP (cn 517675-2), and Y. Miroshnychenko was supported by an EU personal Marie Curie research grant (cn 236417).

References and Notes

1. Y. Kokobun and M. Koshiba, "Novel multi-core fibers for mode division multiplexing: proposal and design principle," IEICE Electron. Express **6**, 522–528 (2009).
2. M. Mansuripur and G. Sincerbox, "Principles and techniques of optical data storage," Proc. IEEE **85**, 1780–1796 (1997).
3. J. W. Nibler and J. J. Yang, "Nonlinear Raman spectroscopy of gases," Annu. Rev. Phys. Chem. **38**, 349–381 (1987).
4. Y. Colombe, T. Steinmetz, G. Dubois, F. Linke, D. Hunger, and J. Reichel, "Strong atom-field coupling for Bose-Einstein condensates in an optical cavity on a chip," Nature **450**, 272–276 (2007).
5. J. Kim and C. Kim, "Integrated optical approach to trapped ion quantum computation," Quantum Inf. Comp. **9**, 181–202 (2009).
6. J. Knudtson and K. Ratzlaff, "Laser beam spatial profile analysis using a two-dimensional photodiode array," Rev. Sci. Instrum. **54**, 856–860 (1983).
7. J. Arnaud, W. Hubbard, G. Mandeville, B. de la Claviere, E. Franke, and J. Franke, "Technique for fast measurement of Gaussian beam parameters," Appl. Opt. **10**, 2775–2776 (1971).
8. M. Giles and E. Kim, "Linear systems approach to fiber characterization using beam profile measurements," Proc. SPIE **500**, 67–70 (1984).
9. P. Shayler, "Laser beam distribution in the focal region," Appl. Opt. **17**, 2673–2674 (1978).
10. P. Brannon, J. Anthes, G. Cano, and J. Powell, "Laser focal spot measurements," J. Appl. Phys. **46**, 3576–3579 (1975).
11. C. Wang, "Measuring 2-D laser-beam phase and intensity profiles: a new technique," Appl. Opt. **23**, 1399–1402 (1984).
12. G. Lim and W. Steen, "Measurement of the temporal and spatial power distribution of a high-power CO_2 laser beam," Opt. Laser Technol. **14**, 149–153 (1982).
13. E. Granneman and M. van der Wiel, "Laser beam waist determination by means of multiphoton ionization," Rev. Sci. Instrum. **46**, 332–334 (1975).
14. S. Sorscher and M. Klein, "Profile of a focussed collimated laser beam near the focal minimum characterized by fluorescence correlation spectroscopy," Rev. Sci. Instrum. **51**, 98–102 (1980).
15. A. Rose, Y. Nie, and R. Gupta, "Laser beam measurement by photothermal deflection technique," Appl. Opt. **25**, 1738–1741 (1986).
16. T. Baba, T. Arai, and A. Ono, "Laser beam profile measurement by a thermographic technique," Rev. Sci. Instrum. **57**, 2739–2742 (1986).
17. D. Marcuse, "Loss analysis of single-mode fiber splices," Bell Syst. Tech. J. **56**, 703–718 (1977).
18. The fiber core acts as an effective "pinhole" for the incoupled into the fiber beam. The image of the pinhole is enlarged in the x direction due to the lensing effect of the fiber wall, but stays unchanged in the y direction. Using ray optics we estimate the enlargement to be n, where $n = 1.46$ is the index of refraction of the fiber glass. The contribution from the lensing effect is fully taken into account in the calibration measurement; see Figs. 4 and 5.